Ferromagnetic layer thickness dependence of the Dzyaloshinskii-Moriya interaction and spin-orbit torques in Pt\Co\AlO$_x$

Cite as: AIP Advances **7**, 065317 (2017); https://doi.org/10.1063/1.4990694
Submitted: 13 April 2017 • Accepted: 23 June 2017 • Published Online: 30 June 2017

R. Lo Conte, G. V. Karnad, E. Martinez, et al.

Ferromagnetic layer thickness dependence of the Dzyaloshinskii-Moriya interaction and spin-orbit torques in Pt\Co\AlO$_x$

R. Lo Conte,[1,2,a] G. V. Karnad,[1,a] E. Martinez,[3] K. Lee,[1] N.-H. Kim,[4] D.-S. Han,[5] J.-S. Kim,[6] S. Prenzel,[1] T. Schulz,[1] C.-Y. You,[4] H. J. M. Swagten,[5] and M. Kläui[1,2,b]

[1]*Johannes Gutenberg-Universität, Institut für Physik, Staudinger Weg 7, 55128 Mainz, Germany*
[2]*Graduate School of Excellence "Materials Science in Mainz"(MAINZ), Staudinger Weg 9, 55128 Mainz, Germany*
[3]*Departamento Fisica Applicada, Universidad de Salamanca, plaza de los Caidos s/n, E-38008 Salamanca, Spain*
[4]*Department of Emerging Materials Science, DGIST, Daegu 42988, Republic of Korea*
[5]*Department of Applied Physics, Center for NanoMaterials, Eindhoven University of Technology, P.O. Box 513, 5600 MB Eindhoven, The Netherlands*
[6]*Research Center for Emerging Materials, DGIST, Daegu 42988, Republic of Korea*

(Received 13 April 2017; accepted 23 June 2017; published online 30 June 2017)

We report the thickness dependence of the Dzyaloshinskii-Moriya interaction (DMI) and spin-orbit torques (SOTs) in Pt\Co(t)\AlO$_x$, studied by current-induced domain wall (DW) motion and second-harmonic experiments. From the DW motion study, a monotonous decay of the effective DMI strength with increasing Co thickness is observed, in agreement with a DMI originating from the Pt\Co interface. The study of the ferromagnetic layer thickness dependence of spin-orbit torques reveals a more complex behavior. The observed thickness dependence suggests the spin-Hall effect in Pt as the main origin of the SOTs, with the measured SOT-fields amplitudes resulting from the interplay between the varying thickness and the transverse spin diffusion length in the Co layer. [http://dx.doi.org/10.1063/1.4990694]

An efficient magnetization manipulation by spin-currents is a key requirement for the design of novel spintronic devices,[1,2] which promise to change the way digital information is processed and stored. In particular, the advantageous scaling of current-induced spin manipulation compared to the Oersted field-induced switching allows for lower power operation at small design rules. Recently, a very efficient current-driven magnetization control has been obtained in multilayer systems with an ultra-thin ferromagnetic layer (FM) sandwiched between two different non-magnetic materials.[3–7] These current-induced torques originate from spin-orbit effects (at least one of the two non-magnetic layers consists of an heavy metal (HM)), so that they are referred to as spin-orbit torques (SOTs).[8] Two different origins have been suggested for the SOTs. One is the spin accumulation induced at the HM\FM interface due to the bulk spin-Hall effect (SHE) in the heavy metal layer.[5,6,9] After being generated, such spin-current diffuses into the ferromagnet, where it interacts with the local magnetization via spin-transfer torque.[10] A second possible origin of the SOTs is the inverse spin-galvanic effect (ISGE),[11,12] which generates a non-equilibrium spin-density at both the top and the bottom interfaces of the ferromagnet. Both effects are expected to induce SOTs whose effective strength is a function of the ferromagnetic layer thickness.

[a]These authors contributed equally
[b]Corresponding author: klaeui@uni-mainz.de

In the same kind of materials stacks the presence of topologically non-trivial spin textures, such as homo-chiral domain walls has been observed.[3,5–7] Chiral domain walls are reported to be very stable against annihilation,[13] thus being promising for technological applications. The origin of these chiral spin structures is the interfacial Dzyaloshinskii-Moriya interaction (DMI),[14–19] an antisymmetric exchange interaction expected to primarily originate from the interface between the heavy metal and the ferromagnet.[18–20] Accordingly, both the DMI and the SOTs are expected to depend strongly on the materials system as well as on the layers thickness, making the study of such dependence a key necessity to reveal the true origin of these effects.

The trilayer Pt\Co\AlO_x has been shown to be a model system with large DMI[21–23] and SOTs,[4,24] however different values have been reported due to the sensitivity of spin-orbit effects to the growth conditions and hence the interfaces. For a thorough understanding of the DMI, SOTs and their origin, a combined-systematic study is required, which has until now been missing.

In this work we provide a complete study of the DMI and the SOTs in identical samples of Pt\Co\AlO_x as a function of the Co layer thickness, combining two key techniques: current-induced DW motion (CIDWM) and second harmonic Hall measurements. Comparing the thickness dependence of the DMI and the torques allows us to draw conclusions about their origins.

The material system studied here is the multilayer: Ta(4.0)\Pt(4.0)\Co(t)\$AlO_x$(2.0) (all thicknesses in nm). The stack is deposited by magnetron sputtering technique on a Si\$SiO_2$ substrate, and has a perpendicular magnetic anisotropy (more info in the supplementary material). Arrays of several nanowires (NWs) in parallel (1.5-2.0 μm in width and 25-28 μm in length, see Fig. 1(a)) are used for CIDWM experiments, while Hall-crosses (1-2 μm in width and 50 μm in length, see Fig. 1(b)) are used for the measurements of effective spin-orbit fields by the second harmonic (2ω) technique.[4,5] During the experiments, the conventional charge current density, $\mathbf{j}_a$, is taken to be positive when it

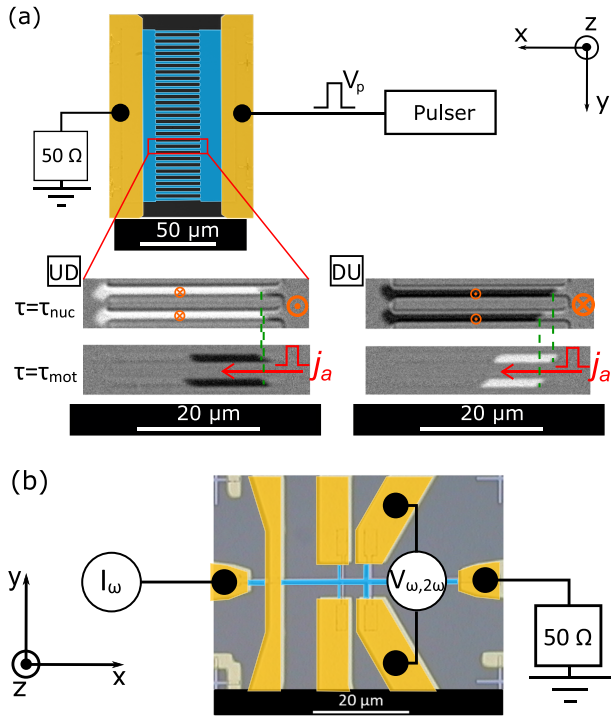

FIG. 1. Experimental setups. (a) Schematic of the experimental setup for CIDWM measurements, including an optical image in false color (blue for the magnetic multilayer, yellow for the Au contacts) of one of the devices. At $\tau = \tau_{nuc}$ the DWs are nucleated in the NWs. At $\tau = \tau_{mot}$ the DWs are moved by the injection of a train of current pulses. The DW displacements are measured by differential Kerr microscopy in the polar configuration. The images show the motion of ↑↓-DWs (UD) on the left and ↓↑-DWs (DU) on the right, respectively. (b) Schematic of the experimental setup for 2ω measurements, including a false colors image of one of the Hall crosses.

flows in the $+x$-direction (see Fig. 1), corresponding to an electron current density, $\mathbf{j}_e$, flowing in the $-x$-direction.

CIDWM experiments are carried out in four different devices, where the nominal thicknesses of the Co layer are: 0.93 nm, 1.31 nm, 1.37 nm and 1.43 nm. The differential Kerr microscopy images in Fig. 1(a) show the current-induced motion for ↑↓ and ↓↑ DWs. The DW type is defined from right to left (+x-axis direction) in Fig. 1(a).

The average DW velocity, v_{DW}, as a function of the current density, j_a, is measured for the four different devices (the $v_{DW} - j_a$ curves are reported in the supplementary material). Both domain wall types (↑↓ and ↓↑) move against the electron flow, which allows to conclude that SOTs are the dominating torques responsible for the DW displacement and that the DWs are all homo-chiral due to the DMI.[5,7]

Next, the DW velocity is measured as a function of an applied magnetic field along the length of the magnetic wires ($\mathbf{H_x}$) for a fixed current density. The measured DW velocities as a function of the longitudinal field, $\mu_0 H_x$, for one of the devices are reported in Fig. 2 (see supplementary material for the other samples). Red (blue) symbols refer to ↑↓- (↓↑-) DWs, while squares (stars) refer to $j_a > 0$ ($j_a < 0$). As visible in Fig. 2, while at zero-field the velocity of both types of DWs is the same, in the presence of a finite longitudinal field the two types of DWs move at different velocities. The change in the field amplitude affects differently the velocity of the two types of DWs, making it possible to obtain ↑↓-DWs and ↓↑-DWs moving in opposite directions, when the field amplitude is large enough. A symmetric behavior is observed for the velocity of the two DW types with respect to H_x, which can be described as: $v_{DW}^{\uparrow\downarrow}(j_a, H_x) = v_{DW}^{\downarrow\uparrow}(j_a, -H_x)$.

Considering an ↑↓-DW, a positive H_x reduces the DW velocity, while a negative H_x increases it. For very large positive H_x the ↑↓-DWs are also observed to change their direction of motion. The opposite field dependence applies to the velocity of ↓↑-DWs.

These observations suggest strong spin-orbit torques acting in the materials stack, in combination with the presence of an interfacial Dzyaloshinskii-Moriya interaction.[5,6,17]

It is known that DMI stabilizes homochiral Néel DWs.[6,7,17,25] This can be interpreted as due to the presence of an effective DMI field, $\mathbf{H}_D$, along the length of the NWs. Accordingly, the stopping field is the field needed to compensate the DMI field and turn the DW into a Bloch configuration, making the spin-orbit torques acting on the DW zero. Therefore, the measurement of the stopping field allows one to estimate the DMI field.

The in-plane field range where DW are pinned can be expressed as: $[-H_D^{\uparrow\downarrow,\downarrow\uparrow} - \Delta H_x{}^{dep}, -H_D^{\uparrow\downarrow,\downarrow\uparrow} + \Delta H_x{}^{dep}]$; where $H_D^{\uparrow\downarrow,\downarrow\uparrow}$ is the DMI effective field for ↑↓, ↓↑ DWs, and $2\Delta H_x{}^{dep}$ is the amplitude of the pinning range. Accordingly, the stopping field can be extracted as the center of the observed pinning ranges of H_x, and so the corresponding H_D. Finally, the strength of the DMI can be obtained from the relation $D = \mu_0 H_D M_s \Delta_{DW}$.[17,26] The described protocol is used to extract the stopping fields for each of the four different DW type (↑↓, ↓↑)-current sign (positive, negative) combinations. For the

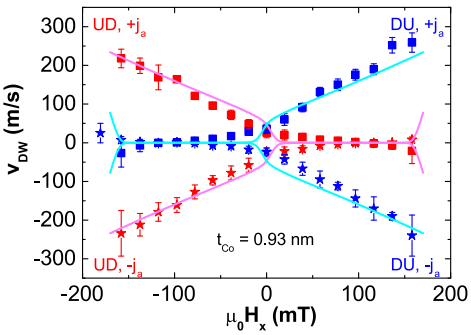

FIG. 2. Average velocity, v_{DW}, of ↑↓ (red symbols) and ↓↑ (blue symbols) DWs as a function of $\mu_0 H_x$, for $j_a > 0$ (squares) and $j_a < 0$ (stars). The average velocities and the error bars (standard deviations) are calculated from several DW motion events for each magnetic field value. The (turquoise and pink) solid lines are the fitting curves obtained by 1D model calculations showing a good agreement with the experimental data. Data for $t_{Co} = 0.93$ nm; $j_a = 8.7 \times 10^{11}$ A/m^2.

magnetic device reported in Fig. 2, with $t_{Co} = 0.93$ nm, an effective DMI field of $\mu_0 H_D = \frac{\mu_0 H_D^{\uparrow\downarrow} - \mu_0 H_D^{\downarrow\uparrow}}{2} = -99 \pm 10$ mT is obtained. After calculating the DW width parameter, $\Delta_{DW} = \sqrt{A/K_{eff}}$, which results to be 3.8 ± 0.1 nm for $t_{Co} = 0.93$nm (exchange stiffness for the Co layer $A = 1.6 \times 10^{-11}$ J/m[17,27]). Accordingly, the effective DMI is $D = -0.54 \pm 0.04$ mJ/m^2. Based on the definition of the DMI Hamiltonian $H_{DMI} = -\mathbf{D} \cdot [\mathbf{S}_i \times \mathbf{S}_j]$, a negative DMI corresponds to the observation of left-handed Néel DWs in our system.

The same process is repeated for $t_{Co} = 1.31$ nm and $t_{Co} = 1.37$ nm, extracting the respective effective DMI field and DMI strength, which are reported in Fig. 3. For the device with $t_{Co} = 1.43$ nm it is not possible to extract a DMI field based on the obtained experimental data, due to a lack of data points in the pinning regime. More details available in the supplementary material.

In multilayer systems such as the one discussed here, the DMI is predicted to originate from the interface between the heavy metal (Pt) and the ferromagnet (Co).[19] Accordingly, the DMI is expected to be an interface-like effect, and its effective (bulk) strength scales with the inverse of the ferromagnetic layer thickness. In Fig. 3 the measured DMI fields (blue diamonds) are shown to be proportional to t_{Co}^{-1}. Furthermore, the extracted values of H_D are in line with what has already been reported in literature for CIDWM experiments on systems with a Pt buffer layer.[6,28] Safeer et al.[28] reported a 100 mT stopping field for DW motion parallel to the current flow in a Pt(3 nm)\Co(0.6 nm)\AlO_x(2 nm) sample. Moreover, Ryu et al.[6] reported a 140 mT stopping field in Pt(1.5 nm)\[Co(0.3 nm)\Ni(0.7 nm)\Co(0.15 nm)] NWs. However, in those previous reports no systematic thickness dependence was provided.

Concerning the extracted DMI strength, the $|D|$ values obtained here are in good agreement with the outcome of other CIDWM-based measurements.[6,28] Furthermore, BLS measurements carried out on the same sample to characterize the DMI showed[23] a decrease of the DMI with increasing Co thickness, when measured across a larger thickness range. This corroborates our experimental observation, and supports our interpretation of DMI being an interface effect. However, the values reported here are found to be quantitatively in disagreement with the values obtained by BLS measurements.[23] This clearly motivates a theoretical analysis about the comparability of DMI measurements obtained with different experimental techniques. Recently, similar differences were also reported by Soucaille et al.,[29] who found that the DMI values extracted separately by DW creep motion studies and BLS measurements on low damping material stacks are different.

To determine the effective SOT-field acting on the DW, a collective-coordinate model (CCM)[25] based on the extension of the one-dimensional model (1DM) is employed to reproduce the experimental observations reported in Fig. 2 (see supplementary material for more details). Due to the secondary role played by the field-like (FL)-SOT on the DW motion,[25] the action of the SOTs on the DW is modeled by the presence of an effective damping-like (DL)-field solely, H_{DW}.

The resulting CCM fitting curves are shown in Fig. 2 and Fig. S3 (solid lines). The corresponding field/current ratio, H_{DW}/j_a, is reported at the top of Fig. 4 as a function of the Co thickness. The extracted effective field is observed to increase for a Co thickness of less than 1.4 nm and then to level off around $H_{DW}/j_a = 5$ [mT/(10^{11}A/m^2)] for larger thicknesses. Furthermore, the sign of the effective field is in agreement with a positive spin-Hall angle (SHA), if the SHE is assumed as the

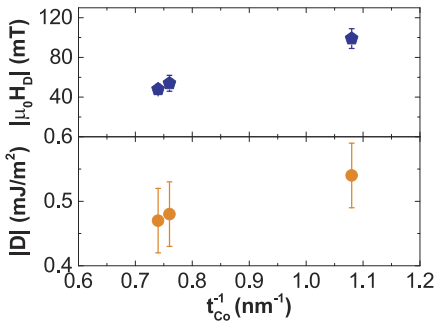

FIG. 3. Thickness dependence of DMI. Extracted effective DMI field, $|\mu_0 H_D|$ (blue diamonds), and extracted DMI coefficients, $|D|$ (orange dots), as a function of the inverse of the Co thickness.

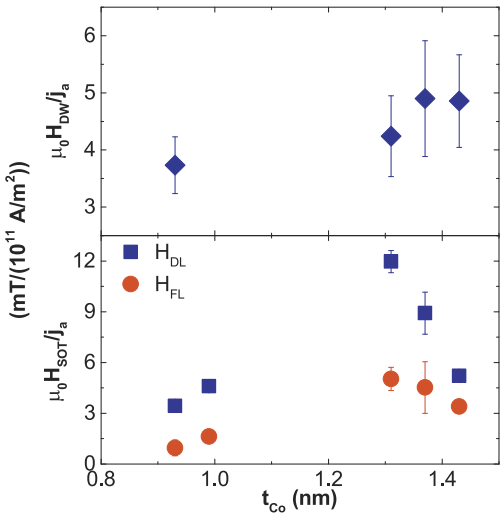

FIG. 4. Thickness dependence of SOT-fields. (Top) Effective SOT-field per current density, H_{DW}/j_a, as extracted by the 1DM calculations that fit the DW motion experiments. The values of H_{DW}/j_a shown here are the ones used for the generation of the fitting curves reported in Fig. 2 and Fig. S3. (Bottom) Field/current ratio for the longitudinal (H_{DL}, blue squares) and transverse (H_{FL}, red dots) effective SOT-field as a function of the ferromagnetic thickness. H_{SOT} defines the general SOT-field.

main source of the observed SOT (see following section for more details), in agreement with previous reports for Pt-based systems.[5,6] The extracted effective SHA values are reported in Fig. S4.

Next, we use the 2ω technique[4,30–32] to study SOTs acting on uniformly magnetized Pt\Co\AlO_x Hall cross devices. The current-induced effective SOT-fields along both the longitudinal (x) and transverse (y) direction are measured (see supplementary material for more details). The effective fields are measured for different devices with a Co thickness of: 0.93 nm, 0.99 nm, 1.31 nm 1.37 nm and 1.43 nm. The experimental results are reported at the bottom of Fig. 4. First, we find that the DL-field is larger than the FL-field. Second, the two effective fields have the same qualitative dependence on the Co thickness, suggesting a possible common origin for the two torques. The two effective fields are observed to first increase and then decrease with the Co thickness, clearly indicating a more complicated character than the one observed for the DMI. Third, the DL-field is found to be always larger than the FL-field, for all the investigated Co thicknesses.

In general, in HM\FM systems the primary origin of the DL-torque is attributed to the SHE due to the large SOC characterizing the heavy metal.[6,24,33] Furthermore, it has been theoretically predicted that the SHE can be the origin of both type of effective fields, with a major contribution to the DL-field, H_{DL}.[34] Accordingly, the spin-Hall effect is likely the dominant source of both SOTs measured here. This conclusions are also in line with what experimentally reported recently by Ou et al.[35]

To understand better the observed thickness dependence, we consider that the ratio H_{DL}/j_a is expected to be proportional to θ_{eff}/t_{FM} (where θ_{eff} represents the efficiency of the SOT).[5,24] In case θ_{eff} is constant with respect to t_{FM}, H_{DL}/j_a scales with $1/t_{FM}$. However, if the SOT efficiency is not constant (as, for example, reported by Pai et al.[36] for ultra-thin ferromagnetic layers) the effective field can actually show a more complex thickness dependence. All this lends itself to the following interpretation: The SHE-induced spin-current diffuses in the ferromagnet and interacts with the local magnetization thus generating the two SOTs.[34] The length scale defining the thickness dependence of the corresponding effective fields is the transverse spin diffusion length (TSDL) in Co,[37] reported to be around 1.2 nm.[38] Indeed, after diffusing across the ferromagnet for a distance equal to the TSDL, the spin-current can be considered absorbed by the ferromagnet and no further effect on the magnetization beyond this thickness is produced. So, in the first TSDL the field/current ratio increases and then decreases with a further increase of the Co thickness.

It is important to note that SOTs due to an ISGE originating at the interface would exhibit a different scaling as a function of the ferromagnet thickness. Furthermore, it has also been

proposed that the ISGE and the DMI can share a common origin,[39,40] and such a common origin for SOTs and DMI was claimed to be present in a Pt\NiFe system.[41] On the contrary, here we directly observe a DMI thickness dependence which is qualitatively different from the one obtained for the effective SOT-fields, demonstrating a different origin for the DMI and the SOTs in our materials system.

In conclusion, the thickness dependence of Dzyaloshinskii-Moriya interaction (DMI) and spin-orbit torques (SOTs) in Pt\Co(t)\AlO_x is characterized. Left-handed homochiral DWs are observed in our system, corresponding to a negative DMI. The extracted DMI decreases in strength with an increasing Co thickness, confirming its interfacial origin. The thickness dependence of the effective SOT-fields is found to be defined by the interplay between the thickness and the transverse spin diffusion length of the Co layer. The qualitatively different dependence of DMI and SOTs on the Co thickness, together with the extraction of a leading DL-SOT suggests that these effects do not share a common origin in the investigated system.

SUPPLEMENTARY MATERIAL

See supplementary material for more details about the materials stack characterization, and for all the remaining graphs describing the outcome of the CIDWM and the 2ω experiments not reported in the main text.

We acknowledge support by the Graduate School of Excellence Materials Science in Mainz (MAINZ) GSC 266, Staudinger Weg 9, 55128 Mainz, Germany; the DFG (KL1811, SFB TRR 173 Spin+X); the EU (IFOX, NMP3-LA-2012 246102; MASPIC, ERC-2007-StG 208162; MultiRev ERC-2014-PoC 665672; WALL, FP7-PEOPLE-2013-ITN 608031) and the Research Center of Innovative and Emerging Materials at Johannes Gutenberg University (CINEMA). E. M. acknowledges the support by project MAT2014-52477-C5-4-P from Spanish government and project SA282U14 from Junta de Castilla y Leon. C.-Y. You and N.-H. Kim acknowledge the support by the National Research Foundation (NRF) of Korea (Grant Nos. 2015M3D1A1070465), the NRF-DFG Collaborative Research Program (No. 2014K2A5A6064900 and No. KL1811/14), and the support by the DGIST R&D Program of the Ministry of Science, ICT and Future Planning (17-BT-02). J.-S. Kim acknowledges the support by the Leading Foreign Research Institute Recruitment Program (No. 2012K1A4A3053565) through the National Research Foundation of Korea.

[1] S. Parkin and S.-H. Yang, Nat. Nanotechnol. **10**, 195 (2015).
[2] A. Fert, V. Cros, and J. Sampaio, Nat. Nanotechnol. **8**, 152 (2013).
[3] I. M. Miron, T. A. Moore, H. Szambolics, L. D. Buda-Prejbeanu, S. Auffret, B. Rodmacq, S. Pizzini, J. Vogel, M. Bonfim, A. Schuhl, and G. Gaudin, Nat. Mater. **10**, 419 (2011).
[4] K. Garello, I. M. Miron, C. O. Avci, F. Freimuth, Y. Mokrousov, S. Blügel, S. Auffret, O. Boulle, G. Gaudin, and P. Gambardella, Nat. Nanotechnol. **8**, 587 (2013).
[5] S. Emori, U. Bauer, S.-M. Ahn, E. Martinez, and G. S. D. Beach, Nat. Mater. **12**, 611 (2013).
[6] K.-S. Ryu, S.-H. Yang, L. Thomas, and S. S. P. Parkin, Nat. Comm. **5**, 3910 (2014).
[7] R. Lo Conte, E. Martinez, A. Hrabec, A. Lamperti, T. Schulz, L. Nasi, L. Lazzarini, R. Mantovan, F. Maccherozzi, S. S. Dhesi, B. Ocker, C. H. Marrows, T. A. Moore, and M. Kläui, Phys. Rev. B **91**, 014433 (2015).
[8] A. Brataas and K. M. D. Hals, Nat. Nanotechnol. **9**, 86 (2014).
[9] J. Sinova, S. O. Valenzuela, J. Wunderlich, C. H. Back, and T. Jungwirth, Rev. Mod. Phys. **87**, 1213 (2015).
[10] D. C. Ralph and M. D. Stiles, J. Magn. Magn. Mater. **320**, 1190 (2008).
[11] V. M. Edelstein, Solid State Commun. **73**, 233 (1990).
[12] S. D. Ganichev, E. L. Ivchenko, V. V. Bel'kov, S. A. Tarasenko, M. Sollinger, D. Weiss, W. Wegscheider, and W. Pretti, Nature **417**, 153 (2002).
[13] M. J. Benitez, A. Hrabec, A. P. Mihai, T. A. Moore, G. Burnell, D. McGrouther, C. H. Marrows, and S. McVitie, Nat. Commun. **6**, 8957 (2015).
[14] I. Dzyaloshinsky, J. Phys. Chem. Solids **4**, 241 (1958).
[15] T. Moriya, Phys. Rev. **120**, 91 (1960).
[16] A. Crepieux and C. Lacroix, J. Magn. Magn. Mater. **182**, 341 (1998).
[17] A. Thiaville, S. Rohart, É. Jué, V. Cros, and A. Fert, Europhys. Lett. **100**, 57002 (2012).
[18] V. Kashid, T. Schena, B. Zimmermann, Y. Mokrousov, S. Blügel, V. Shah, and H. G. Salunke, Phys. Rev. B **90**, 054412 (2014).
[19] H. Yang, A. Thiaville, S. Rohart, A. Fert, and M. Chshiev, Phys. Rev. Lett. **115**, 267210 (2015).
[20] H. T. Nembach, J. M. Shaw, M. Weiler, E. Jué, and T. J. Silva, Nat. Phys. **11**, 825 (2015).
[21] M. Belmeguenai, J.-P. Adam, Y. Roussigné, S. Eimer, T. Devolder, J.-V. Kim, S. M. Cherif, A. Stashkevich, and A. Thiaville, Phys. Rev. B **91**, 180405 (2015).

[22] J. Cho, N.-H. Kim, S. Lee, J.-S. Kim, R. Lavrijsen, A. Solignac, Y. Yin, D.-S. Han, N. J. J. van Hoof, J. M. Swagten, B. Koopmans, and C.-Y. You, Nat. Commun. **6**, 7635 (2015).
[23] N.-H. Kim, D.-S. Han, J. Jung, J. Cho, J.-S. Kim, H. J. M. Swagten, and C.-Y. You, Appl. Phys. Lett. **107**, 142408 (2015).
[24] L. Liu, O. J. Lee, T. J. Gudmundsen, D. C. Ralph, and R. A. Buhrman, Phys. Rev. Lett. **109**, 096602 (2012).
[25] E. Martinez, S. Emori, N. Perez, L. Torres, and G. S. D. Beach, J. Appl. Phys. **115**, 213909 (2014).
[26] S. Emori, E. Martinez, K.-J. Lee, H.-W. Lee, U. Bauer, S.-M. Ahn, P. Agrawal, D. C. Bono, and G. S. D. Beach, Phys. Rev. B **90**, 184427 (2014).
[27] A. Hrabec, N. A. Porter, A. Wells, M. J. Benitez, G. Burnell, S. McVitie, D. McGrouther, T. A. Moore, and C. H. Marrows, Phys. Rev. B **90**, 020402(R) (2014).
[28] C. K. Safeer, E. Jue, A. Lopez, L. Buda-Prejbenau, S. Auffret, S. Pizzini, O. Boulle, I. M. Miron, and G. Gaudin, Nat. Nanotechnol. **11**, 143 (2016).
[29] R. Soucaille, M. Belmeguenai, J. Torrejon, J.-V. Kim, T. Devolder, Y. Roussigne, S. M. Cherif, A. A. Stashchevich, M. Hayashi, and J.-P. Adam, Phys. Rev. B **94**, 104431 (2016).
[30] U. H. Pi, K. W. Kim, J. Y. Bae, S. C. Lee, W. J. Cho, K. S. Kim, and S. Seo, Appl. Phys. Lett. **97**, 162507 (2010).
[31] M. Hayashi, J. Kim, M. Yamanouchi, and H. Ohno, Phys. Rev. B **89**, 144425 (2014).
[32] H.-R. Lee, K. Lee, J. Cho, Y.-H. Choi, C.-Y. You, M.-H. Jung, F. Bonell, Y. Shiota, S. Miwa, and Y. Suzuki, Sci. Rep. **4**, 6548 (2014).
[33] L. Liu, C.-F. Pai, Y. Li, H. W. Tseng, D. C. Ralph, and R. A. Buhrman, Science **336**, 555 (2012).
[34] P. M. Haney, K.-J. Lee, H.-W. Lee, A. Manchon, and M. D. Stiles, Phys. Rev. B **87**, 174411 (2013).
[35] Y. Ou, C.-F. Pai, S. Shi, D. C. Ralph, and R. A. Buhrman, Phys. Rev. B **94**, 140414(R) (2016).
[36] C.-F. Pai, Y. Ou, L. H. Vilela-Leao, D. C. Ralph, and R. A. Buhrman, Phys. Rev. B **92**, 064426 (2015).
[37] A. Shpiro, P. M. Levy, and S. Zhang, Phys. Rev. B **67**, 104430 (2003).
[38] A. Ghosh, S. Auffret, U. Ebels, and W. E. Bailey, Phys. Rev. Lett. **109**, 127202 (2012).
[39] K.-W. Kim, H.-W. Lee, K.-J. Lee, and M. D. Stiles, Phys. Rev. Lett. **111**, 216601 (2013).
[40] F. Freimuth, S. Blügel, and Y. Mokrousov, J. Phys.-Condens. Mat. **26**, 104202 (2014).
[41] A. J. Berger, E. R. J. Edwards, H. T. Nembach, J. M. Shaw, A. D. Karenowska, M. Weiler, and T. J. Silva, arXiv:1611.05798v1 (2016).